Fracture Mechanics of Concrete Structures
Proceedings FRAMCOS-3
AEDIFICATIO Publishers, D-79104 Freiburg, Germany

CHARACTERIZATION OF INTERFACE FRACTURE BEHAVIOR IN REPAIRED CONCRETE INFRASTRUCTURES

Y. M. Lim
Applied Mechanics Laboratory, Civil Engineering Department,
School of Civil and Urban Engineering,
Yonsei University, Seoul (120-749), Korea
V. C. Li
Advanced Civil Engineering Material Research Laboratory,
Department of Civil and Environmental Engineering,
The University of Michigan, Ann Arbor, MI 48109, U.S.A.

Abstract

Usually repair systems can be divided into three different phases of materials -- repaired substrate phase, repair material phase and the interface phase between substrate and repair material. Each phase of material has to have its own role in the system for durable repair. Among the three phases, the interface phase especially has the most important role to integrate the repair systems. Recently, interface properties -- bond strength and interface fracture toughness, etc. -- were focused on to predict the performance of repair systems. In this paper, the interface between old concrete as a repaired substrate and repair material based on cementitious composites is characterized using interface fracture mechanics. The interface fracture toughness is experimentally measured with three potential repair materials -- plain concrete, steel fiber reinforced concrete (FRC), and engineered cementitious composite (ECC). Furthermore this measured interface property is utilized theoretically to predict the interface fracture behavior. Based on this prediction, a trapping mechanism is discovered and this mechanism is experimentally demonstrated in representative repaired concrete infrastructures to show stronger, more ductile, and more energy absorbing repair system in comparison to the other potential repair systems.

Key words: durable repair, interface property, interface fracture toughness, trapping mechanism

1 Introduction

For durable repair of aged concrete infrastructures, the interface property is considered an important parameter (Deming et al., 1994; Li et al., 1995). Tensile or shear bond strength is usually accepted as an interface property in practice accompanied by a variety of test techniques (Emmons, 1994). This bond strength may be useful for ranking of repair materials, but is not expected to have field performance predictive capability due to size and geometric effects. On the other hand, interface fracture toughness is considered an interface property capable of predicting repair system performance associated with interface crack extension (Lim and Li, 1997).

Various experimental methods to measure the interface fracture toughness have been developed. A pre–notched bending specimen with symmetric and asymmetric loading configurations is selected to measure interface fracture toughness with various mode mixity in interface systems which have a concrete substrate and three potential repair materials (Lim, 1996). This measured interface fracture toughness is utilized to predict the interface crack propagation along the interface or kinking out from the interface.

The major objective of this paper is characterization of interface fracture behavior in repaired concrete infrastructures through the interface fracture toughness measurement and utilization of this characteristics to predict the cracking behavior in a representative repair system designed for laboratory scale test. This research can provide a new methodology of repair material design and selection with the consideration of interface fracture behavior.

2 Experimental Programs

2.1 Set–up of interface fracture toughness test

Many different experimental set–ups have been developed to measure interface fracture toughness at different phase angles (Cao and Evans, 1989; Charalambides et al., 1989; Wang and Suo. 1990). Some set–ups designed to measure at a fixed phase angle, while others have the capability to measure with varied phase angles. In this study, a bending specimen set–up with symmetric and asymmetric loading configurations is selected. The main reason why these set–ups are selected are (i) these set–ups are relatively easy to handle, (ii) the set–ups afford a large range of phase angles with only a single specimen geometry, and (iii) the calibration functions for varied material combinations have already been developed.

Fig. 1 schematically shows the loading arrangement, and the variation

of the shear force (SFD) and bending moment (BMD) along the length of the specimen. The symmetric set–up in Fig. 1 (a) is used for approximately zero degree phase angle. The asymmetric set-up in Fig. 1 (b) is used for various phase angle with varying offset s. The offset s is measured from the center of loading line to the interface.

2.2 Specimen design

In this study, two different specimen shape are developed to measure interface fracture toughness in the interface system between concrete and cementitious composites (Fig. 2).

The uniform thickness specimen was developed at the beginning of this experimental program. At that time, there was no information about interface fracture toughness in concrete/cementitious composite interface systems. Thus, the capacity of this uniform thickness specimen could not be estimated. These specimens performed well at phase angles less than 45°. However, at phase angles greater than 45°, interface fracture toughness is found to rapidly increase, and the specimens then failed by flexure in either material.

To prevent this unexpected failure, a varied thickness specimen was developed (see Fig. 2 (b)). The bending capacity at the maximum bending moment area in the varied thickness specimen is improved about 3.5 times compared with that of the uniform thickness specimen. This improvement prevents the flexural failure at the maximum bending moment point. The thickness at the middle of the specimen remains the same as the thickness

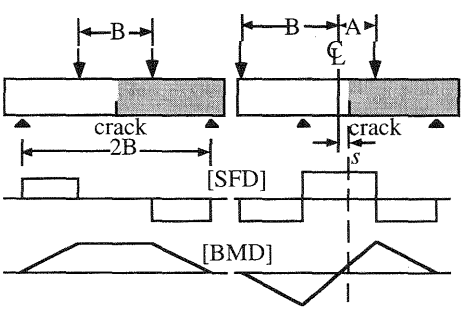

(a) Symmetric set–up (b) Asymmetric set–up

Fig. 1 Set–ups and loading configuration

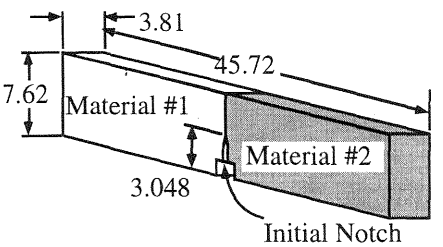

(a) Uniform thickness

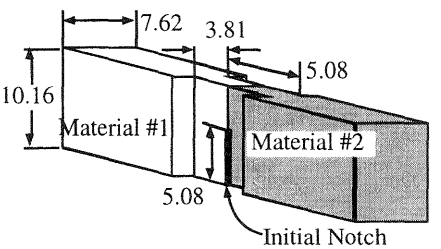

(b) Varied thickness

Fig. 2 Type of specimens (cm)

of the uniform thickness specimen. Thus, the stress field at the crack tip is not changed by the change of specimen types (O'Dowd et al., 1992). The difference of the measured toughness due to the change of the specimen types is negligible (Lim, 1996).

2.3 Specimen preparation

The casting methods of those two beams are illustrated in Fig. 3 and Fig. 4. The substrate material was cast and cured five weeks (4 weeks water curing and 1 week air drying), and then the repair material was cast against the substrate material. The complete interface specimens were cured two more weeks under water before testing. This substrate material imitates the substrate material in aged infrastructures. All specimens were cured under the same curing conditions.

In the uniform thickness specimen, the substrate material was horizontally cast with a "notch maker" in the left hand side of the mold with divider (Fig. 3 (a)). The repair material was then cast on the right hand side of the mold with the base material (Fig. 3 (b)). The interface surface in the substrate material was ground using a bench grinder to remove contamination from demolding oil and hydration product against the mold prior to casting the repair material. As a result of this grinding, some aggregates were slightly exposed and the grinding surface was smooth.

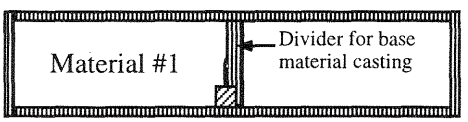

(a) Casting method

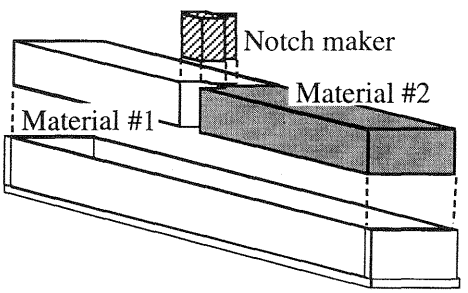

(b) Casting for bimaterial

Fig. 3 Casting method in uniform thickness specimens

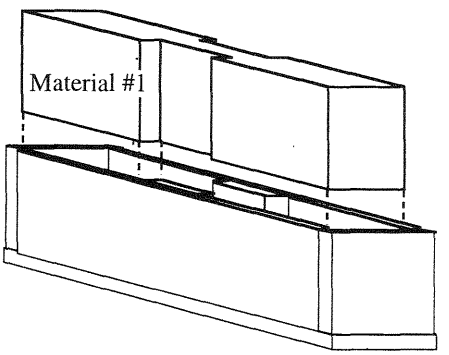

(a) Casting method

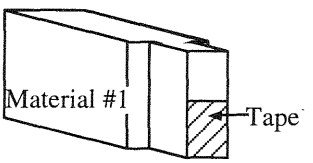

(b) Method of notch making

Fig. 4 Casting method in varied thickness specimens

In the varied thickness specimens, the substrate material was vertically cast (Fig. 4 (a)). The substrate material was cut in half using a diamond saw approximately five hours before the repair material casting. A tape with very smooth surface was partially attached on the cut surface of base material (see Fig. 4 (b)), and it functions as a sharp notch in the bimaterial specimens. Half of the cut substrate material was placed back into the mold and the repair material was cast on the right hand side.

2.4 Materials

Three different repair materials were cast and tested with base concrete. For the base concrete, 28 MPa compressive strength concrete at 7 weeks old, including one week drying, was used. The mix design followed ACI recommendations.

For the repair materials, concrete, FRC, and ECC were used. For the repair concrete, the same concrete with substrate was used. In FRC, hooked–end steel fibers (ZL 30/50) were mixed at 1% volume fraction. The diameter and length of this steel fiber are 0.5 mm and 30 mm, respectively. The ECC contains a 2% volume fraction of Spectra 1000 fibers (high modulus polyethylene fibers) with 28 μm diameter and 12.7 mm length. Table 1 contains the material mix proportions. Standard river sand and crushed stone were used in this mix design for the base concrete, repair concrete, and FRC.

Table 1. Material mix design by solid contents

Material	PC	water	FA	CA	SF	SP	Fiber*
Concrete	1.0	0.5	2.27	1.8	-	-	-
FRC	1.0	0.5	2.27	1.8	-	-	0.01
ECC	1.0	0.35	0.5**	-	0.1	0.017	0.02

(PC: Portland Cement Type I; FA: Fine Aggregate; CA: Coarse Aggregate < 9.5 mm; SF: Silica Fume; SP: Super Plasticizer; * volume fraction; ** 50-70 Silica Sand)

3 Critical energy release rate

3.1 Measurement and calibration

The bimaterial bending specimens were removed from water and allowed to dry for 24 hours before testing. The specimens were then tested under displacement control at a rate of 0.005 mm/sec in a closed-loop MTS loading frame.

The calibration for this interface specimen was developed based on a finite element analysis assuming linear elastic material behavior (O'Dowd et al., 1992). Load–deflection in cementitious interface systems shows

almost linear behavior up to the failure point (Lim, 1996). The inelastic zone of the interface crack tip might be small enough to consider linear elastic fracture mechanics (LEFM) since there is no aggregate interlocking or fiber bridging across the interface. Thus, a fully elastic calibration function can be used to interpret the interface fracture toughness (Hutchinson and Suo, 1992).

3.2 Experimental results

In most cases of the interface fracture toughness tests, the load–deflection curves show one steep load drop after the first interface cracking, suggesting that the interface crack propagates rapidly once initiated, and completely ruptures the specimens. Even if there is post–peak behavior, the second and third peak load usually are negligible.

Four different failure modes were found in this interface fracture toughness test (Fig. 5). In the first, the interface crack clearly propagates along the interface with only small remnants of adjoining material remaining on the interface fracture surface (mode A). In the second mode, the interface crack propagates along the interface for approximately 2/3 of the remaining beam depth, at which point the crack kinks out to the repair material (mode B). This may be due to the stress field changes as the interface crack approaches the upper beam surface, but the second load peak due to this kinking is negligible in most cases. In the third mode, the interface crack propagates along the interface slightly (around 3–5 mm) and kinks out from the interface (mode C). This failure mode usually occurs with a phase angle greater than 60°. Finally, the interface crack can directly kink out from the initial notch tip to the repair material (mode D). This case is not considered as an interface fracture and is not included in the evaluation of interface fracture toughness.

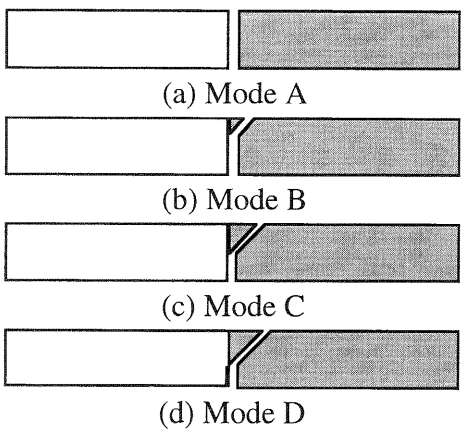

Fig. 5 Failure mode

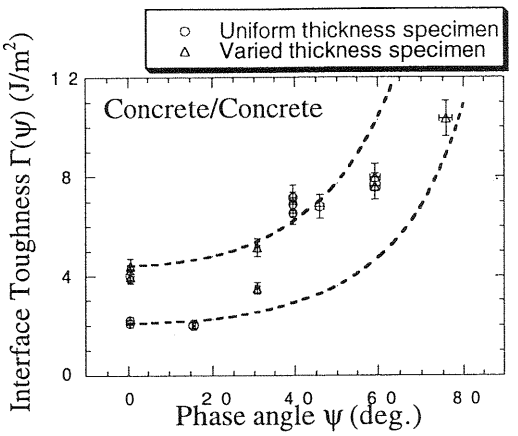

Fig. 6 Interface fracture toughness in concrete/concrete system

The typical error bar represented in Fig. 6, 7 and 8 contains the load–cell sensitivity (±1%), the measuring error of geometric dimensions A, B, and s (±0.3 mm), and the variation of beam thickness (<2%). Also, two dashed curves (upper and lower bounds) in Fig. 6, 7, and 8 are the best fitted curve by eyes using the empirical fitting curve suggesting by Hutchinson and Suo (1992).

3.2.1 Concrete/concrete interface system

In a concrete/concrete interface system, the measured interface fracture toughness Γ with varied phase angles ψ ranging from 0° to 75° is illustrated in Fig. 6. The results of two different types of specimens are reported in the same graph. The uniform thickness specimens and the varied thickness specimens can provide results up to about 45° and about 75°, respectively. The difference between these two types of specimens is negligible, since the thickness change in the varied thickness specimens is far enough from the crack tip.

At phase angles of about 0°, 15°, and 30°, the specimens commonly fail with failure mode A. On the other hand, failure mode B is dominant at phase angles from 40° to 60°. Only one specimen was successfully tested at a phase angle of 75° with failure mode C. Two specimens at a phase angle of 75° failed with failure mode D with low ultimate capacities, and these data are not included.

3.2.2 Concrete/FRC interface system

The interface fracture toughness of concrete/FRC interface systems with varied phase angles is slightly higher than that of concrete/concrete interface system. This trend is consistent with bond strength measurements in carbon and steel micro fiber composites as a repair

material (Banthia and Dubeau, 1994). A possible mechanism of this phenomenon is that fibers reduce the size of flaws developed by shrinkage at the bimaterial interface.

Failure mode A is dominant with the phase angle less than 30°. A uniform thickness specimen was tested at phase angle 45°, but it failed by flexure. So two specimens were tested at phase angle 40° rather than 45°. Those two specimens showed failure mode A and failure mode C with 1/3 of interface crack propagation.

At phase angles 60° and 75° with varied thickness specimens, failure mode C with about 2–3 mm interface cracking was observed. The post-peak load is usually lower than the first peak loading even with the bridging effect of steel fibers. However, in a specimen at a phase angle of 60°, the post-peak loading is higher than the first peak loading due to the bridging effect of steel fibers. In this case, a non-uniform fiber dispersion might be the reason of this exceptional experimental result.

3.2.3 Concrete/ECC interface system

Fig. 8 illustrates the interface fracture toughness of the concrete/ECC interface system computed based on the first load drop in the load-deflection curve. The interface fracture toughness of concrete/ECC interface system is significantly improved compared with that of concrete/concrete interface system at whole range of the tested phase angle. The mechanism of this improvement is not understood at present. All specimens at phase angles of about 5°, 20°, and 35° showed the failure mode B with 80% interface cracking with post peak behavior carrying capacity of about 25% of the first peak capacity.

For specimens tested at a phase angle of 47° (two specimens), the effect of ECC is particularly pronounced. These two specimens showed failure mode C with higher post-peak behavior. The interface crack started to propagate along the interface and the crack tip kinked into the ECC material to initiate the pseudo strain-hardening of the ECC, allowing the load to grow high enough to eventually break the uniform thickness specimen in flexure in the base concrete.

The varied thickness specimen at the phase angle 60° also showed failure mode C. The interface crack initially propagated about 3 mm along the interface and kinked into the ECC. The kinked crack was stopped in the ECC prior to development of several adjacent micro–cracks parallel to the first kinked crack, and then the interface crack propagated again about 12 mm along the interface. This interface crack kinked again into the ECC and was trapped again in the ECC. This phenomenon (sequential kinking, trapping and interface cracking) is further discussed in the following section.

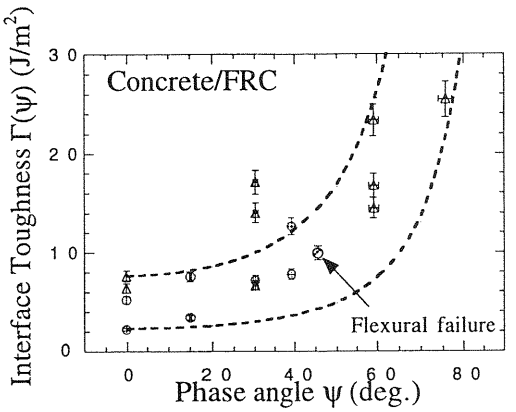

Fig. 7 Interface fracture toughness in concrete/FRC system

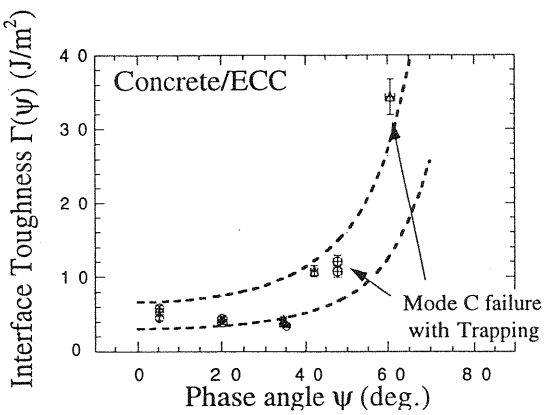

Fig. 8 Interface fracture toughness in concrete/ECC system

4 Trapping mechanism of interface crack

Delamination and spalling are commonly observed in repaired structures such as repaired pavements, bridge decks, and parking structure slabs. One technique to overcome these failure modes in a repair system is to induce kinking when the system is overloaded, followed by arrest of the kink–crack inside repair material as shown in concrete/ECC interface system in the last section. We call this the *interface crack trapping mechanism* (Lim and Li, 1997). This trapping mechanism can be achieved by employing a well–designed ECC as the repair material.

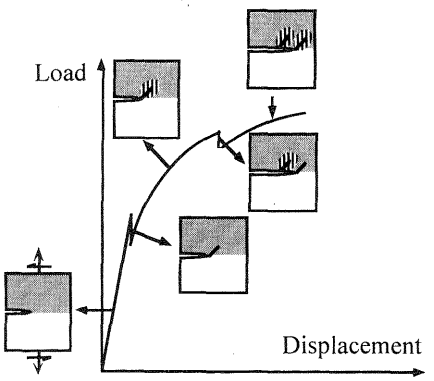

Fig. 9 Trapping mechanism

4.1 Concept of trapping mechanism

Interface crack can kink into repair material when the crack–tip satisfies the "interface crack kink condition" which has two terms -- relative driving force and relative toughness terms (Hutchinson and Suo, 1992). The relative driving force can be analytically or numerically calculated and the relative toughness should be evaluated from experimental measurement of the interface toughness and the toughness of the repair material. From the previous study (Lim, 1996), a low initial fracture toughness with a rapid rise R-curve behavior of repair material or a low first crack strength with a large margin to ultimate tensile strength is the essential requirements of the trapping mechanism in a repair system. ECC is the one which is satisfy these trapping mechanism requirements. Fig. 9 shows the conceptual trapping mechanism with load–displacement relation. Large amount of energy dissipation is expected during the sequence of kinking, damaging, trapping, and interface crack propagation.

4.2 Verification of the trapping mechanism

To verify the trapping mechanism, a typical repair system is selected in this study. In many cases, reflective cracking in the repair material above a joint in the original pavement system is a commonly observed phenomenon of overlay failure. The specimens in this study induce a defect in the form of an interfacial crack between the repair and the concrete substrate, as well as a joint in the substrate. Three different potential repair materials are also used in this test. The shape and loading condition of specimens have the phase angle around 41°~45°, and this phase angle range is within the transition between interface and kink crack propagation.

As expected, only ECC repair system shows the trapping mechanism with superior energy absorption capacity (Fig. 10). The area under load–defection curve of the ECC overlay system is about 2~4 and 35~107 times lager than those of the FRC and concrete overlay systems respectively.

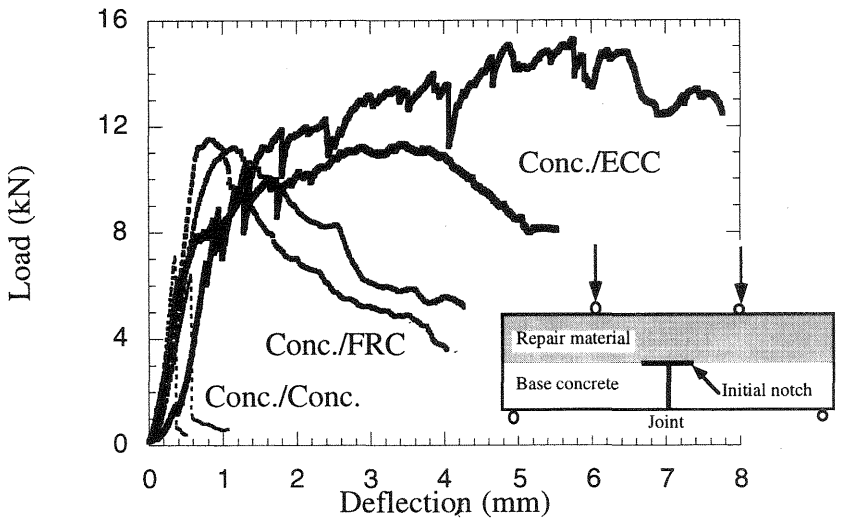

Fig. 10 Load–defection behavior in overlay systems

This remarkable improvement of energy absorption capacity in the ECC overlay system can provide the safe behavior of rehabilitated infrastructures under impact or high energy input load.

5. Conclusions

Interface fracture toughness in different cementitious repair systems was experimentally measured for the characterization of interface fracture behavior in repaired systems. The measured interface fracture toughness values were found to increase with increasing phase angles up to 75° (maximum phase angle in test). Increase in interface fracture toughness with phase angle up to about 8 times was found, depending on the type of repair material. This measured interface property used for the prediction of interface fracture behavior (interface crack propagation along the interface or kink out from the interface).

The concept of interface crack trapping mechanism in the concrete/ECC system was introduced. The presence of this trapping mechanism is confirmed in experimental investigations involving specimens resembling bonded pavement overlay system. The trapping behavior cannot be found in the other overlay systems (the concrete and the FRC overlay systems). The overlay system with trapping mechanism can prevent the most common failures in rehabilitated infrastructures such

as spalling and delamination of repair part with superior energy absorption capacity.

Thus, the repair system with trapping mechanism can achieve durable repair in aged infrastructures by eliminating interface defect induced failure. This achievement cannot be possible without the characterization of interface fracture behavior.

6. References

Banthia, N. and Dubeau, S. (1994) Carbon and steel microfiber reinforced cement based composites for thin repair. **J. of Materials in Civil Engineering**, ASCE, 6(1), 88-98.

Cao, H. C. and Evans, A. G. (1989) An experimental study of the fracture resistance of bimaterial interface. **Mechanics of Materials**, 7, 295-304.

Charalambides, P. G., Lund, J., Evans, A. G. and McMeeking, R. M. (1989) A test specimen for determining the fracture resistance of bimaterial interfaces. **J. of Applied Mechanics**, 56, 77-88.

Deming, B.M., Aktan, H. and Usmen, M (1994) Test for polymer overlay interface on concrete, in **the Third Materials Engineering Conference, Infrastructures: New Materials and Methods of Repair** (ed. Basham, K. D.), ASCE, San Diego, CA, 709-715.

Dundurs, J. (1969) Edge–bonded dissimilar orthogonal elastic wedges. **J. of Applied Mechanics**, 32, 400-402.

Emmons, P. H. (1994) **Concrete repair and maintenance illustrated**. Concrete Publisher & Consultants, Kingston.

Li, V. C., Lim, Y. M. and Foremsky, D. J. (1995) Interfacial fracture toughness of concrete repair materials, in **FRAMCOS-2, Fracture Mechanics of Concrete Structures** (ed. F. H. Wittmann), AEDIFICATIO Publishers, Freiburg, Germany, 1329-1244.

Lim, Y. M. (1996) **Interface Fracture Behavior of Rehabilitated Concrete Infrastructures using Engineered Cementitious Composites**. Ph.D. Thesis, The University of Michigan, Ann Arbor.

Lim, Y. M. and Li, V. C. (1997) Durable repair of aged infrastructures using trapping mechanism of engineered cementitious composites. **J. Cement and Concrete Composite**, 19(4), 373-385.

Wang, J. S. and Suo, Z. (1990) Experimental determination of interfacial toughness using Brazil-nut-sandwich. **Aca Met.**, 38, 1279-1290.